

# Modeling Fluid-Structure Interaction in Cavitation Erosion using Smoothed Particle Hydrodynamics

Shrey Joshi<sup>1,2</sup>, Jean Pierre Franc<sup>2</sup>, Giovanni Ghigliotti<sup>2</sup>, Marc Fivel<sup>1</sup>

<sup>1</sup>*Univ Grenoble Alpes, CNRS, Grenoble INP, SIMaP, 38000 Grenoble, France*

<sup>2</sup>*Univ. Grenoble Alpes, CNRS, Grenoble INP, LEGI, 38000 Grenoble, France*

## Abstract

In the present study a meshless Smoothed Particle Hydrodynamics cavitation solver is developed. The fluid bubble collapse solver is validated against analytical Rayleigh-Plesset equation and shows good agreement. The solid solver capable of solving elastic-plastic deformation and material damage is developed and is validated against FEM results. A fluid structure interaction solver capable of solving cavitation erosion is presented. A single bubble collapse is demonstrated in the paper.

**Keywords:** Smoothed Particle Hydrodynamics, fluid-structure interaction, cavitation, material damage

## Introduction

Cavitation erosion is a major issue amongst a wide range of equipment such as hydraulic devices, diesel injectors, artificial heart valves etc. Cavitation is defined as the appearance of vapour cavities inside a continuous and homogeneous liquid medium. The generation of vapour cavities could happen due to various reasons, but the cause is mostly associated to the drop of local pressure below the vapour pressure. During cavitation the continuum liquid medium breaks down to form vapour cavities. The vapour formation occurs in cavitation when the pressure drops below the vapour pressure as the new pressure and temperature lies in the vapour phase zone.

These vapour bubbles can collapse when the ambient pressure increases above the vapour pressure. The collapse of these bubbles can be very different depending on the position of the bubbles wrt to a solid surface. A collapse of bubble near the surface can lead to formation of a high velocity micro jet and subsequent shock wave. The asymmetric collapse in presence of the wall near the bubble is due to the lack of fluid flow from the side of the wall. This micro-jet then hits the other side of the bubble producing an intense shock wave. The solid surface experiences a high pressure due the shock wave and the high velocity micro jet hitting the surface. The magnitude of the pressure acting on the surface could be high enough to cause plastic damage in the material. Although the experimental measurement of these pressures acting on the surface still remains a challenge, various studies have estimated it to be around a few GPa [1-5]. Moreover, experimental investigation offers only limited information about bubble collapse and the subsequent formation of micro jet and pressure wave since any intrusive measurement can cause deviations. Such difficulties in experimental investigation has led to the use of numerical studies to understand and analyze cavitation.

A thorough cavitation study requires a two-way fluid-structure interaction coupling to get realistic results for cavitation erosion. A comprehensive cavitation numerical model should include the following elements in the solver:

- A fluid model capable of capturing the dynamics of a collapsing bubble including the details about the micro-jet and the shock wave.
- A solid solver to solve for the material response due to the pressure acting on the material surface as a result of the micro jet and the shock wave. This solver must be capable of solving an elastic-plastic behavior as well as damage in the material.
- A fluid structure interaction solver: During a cavitation bubble collapse, high intensity shock waves are produced along with micro-jet. The shock wave travels through the fluid to the solid, a part of the wave is reflected back into the liquid and the rest gets transmitted to the solid [6]. In the case of two elastic media, transfer of the energy and the solid-liquid interface velocity depends on the ratio of acoustic impedances of

the liquid and solid. Acoustic impedance could be estimated simply as the product of density by the speed of sound through the medium. A two-way coupling is required to model this behavior properly.

Conventionally, ALE (Arbitrary Lagrangian Eulerian) methods have been used to simulate such a problem. The problem is quite complex since the fluid solver (Finite Volume Method (FVM) code) and a solid solver (Finite Element Method (FEM) code) are generally two different codes which then need to be coupled in order to communicate data across the two solvers. To overcome the above complexity, in the present study a first attempt has been made to solve cavitation using a meshless method Smoothed Particle Hydrodynamics (SPH). The method offers the following advantages:

- Both fluid and solid response can be captured using the same solver and the same numerical method i.e. SPH, hence eliminates the use of two different solvers while numerically solving for cavitation.
- Coupling an FVM solver to an FEM solver can be quite complicated and requires a coupling for data transfer across the two codes. The problem is eliminated as the solver uses SPH for both solid and fluid and no such coupling is required.
- The material can exhibit plastic deformation during cavitation, while using mesh methods would require a mesh re-construction algorithm to account for the deformed material. The reconstruction of mesh for fluid is required which is complex and can slow the code significantly. However, this problem is eliminated while using meshless methods like SPH.

### Axisymmetric SPH solver

In the present work a 2D axisymmetric Smoothed Particle Hydrodynamics solver is developed. An existing fluid 2D SPH solver SPHYSICS [7] is used as the basis to develop the solver further. For a 2D axisymmetric fluid solver the cylindrical form of SPH equations are used [8] and the original solver is modified accordingly. A cavitation bubble collapse simulation was carried out. Figure 1 shows the domain used for a bubble collapse simulation in an infinitely large medium. The wave maker shown in the figure is a set of repulsive particles in SPH which apply force on the nearby particles hence acting as a pressure wave generator. Figure 2 shows the comparison for a bubble collapse radius wrt time against 3D Rayleigh-Plesset equation which shows good agreement.

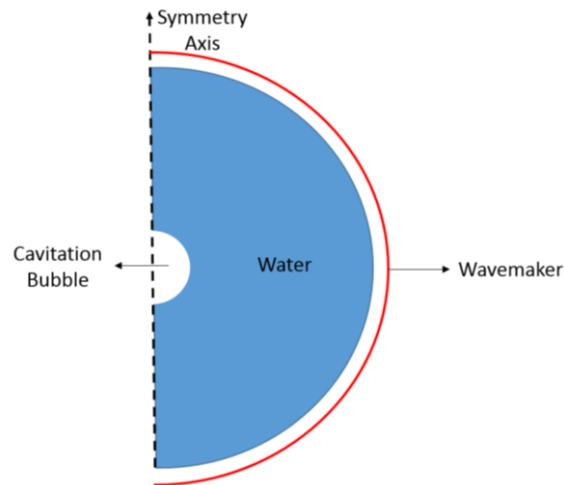


Figure 1. Simulation domain for bubble collapse simulation in 2D axisymmetric, a vacuum bubble of radius 0.095 mm is placed in a spherical domain which is 7 times the bubble radius. A pressure wave of 60 MPa is generated by the wavemaker whereas the initial pressure inside the bubble is 0 Pa, all the domain walls are given a non-reflective boundary condition to avoid any wave reflections hitting the bubble. The flow is treated as non-viscous and no surface tension forces are considered in the model.

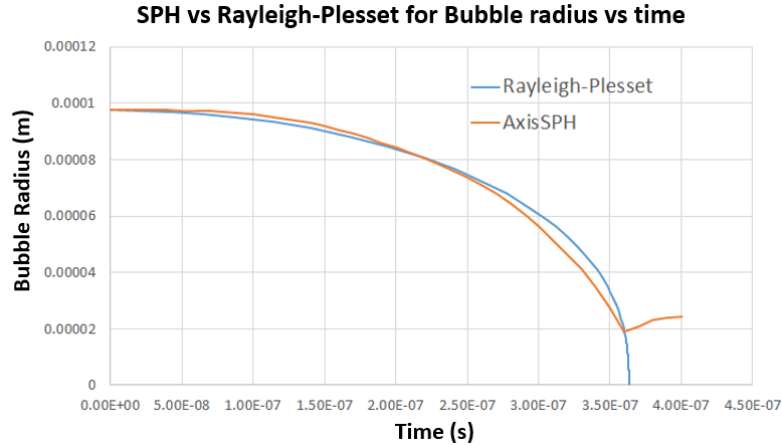


Figure 2. Comparison of bubble radius vs. time, SPH against Rayleigh-Plesset solution for a bubble collapse simulation (domain shown in figure 1).

For the solid SPH solver, similar to the fluid solver the momentum equations are modified to cylindrical SPH equations. However, the additional terms due to density correction near axis have only been derived for a fluid solver [8]. For a similar density correction, a novel scheme is implemented with new momentum equation for a solid with additional terms occurring due to density corrections. Plasticity behavior is modelled using Yield criteria from Johnson-Cook model [9]. The elastic-plastic solver is then validated against FEM (obtained from FEM solver Castem [11]) results for an indentation simulation. Figure 3 shows the domain used for indentation simulations, the boundary particles are given a downward velocity to produce an indent in the solid specimen. Figure 4 shows comparison between SPH and FEM solvers which shows an excellent agreement. The solid SPH solver is thus validated.

To account for mass loss a damage criterion is to be introduced into the model. A simple damage criterion based on the plastic strain is used in the present simulations. A critical value of fracture strain is used to predict whether the SPH particle is damaged or not. If the plastic strain is above the fracture strain the material can sustain, the particle is assumed damaged and removed from the simulation. The material used for simulation is stainless steel A-2205 with fracture strain ( $\epsilon_f$ ) 0.03. Figure 5 shows a sequence of images showing the evolution of damage for one single indentation. Further simulations were carried out to understand the effect of indenter size (that might to some extent correspond to bubble size) while keeping the indentation depth unchanged and the results are shown in figure 6. The graph on figure 6 shows that the larger radius of indenter can produce high mass loss rate but the incubation time appears to be smaller for smaller indenter which is counter-intuitive. The reason is that the plastic deformation has a direct dependence on von Mises stress and the smaller radius indenter can produce significantly higher shear stress compared to the larger radius indenter for the same depth of indent, the von Mises stress is thus higher in case of smaller indenter leading to lower incubation time. However, the larger indenter can plastify a larger volume of the specimen and hence could produce higher mass loss rates over a longer period of time.

The two solvers i.e. the fluid SPH and the solid SPH solvers have been separately validated and used to produce mass loss curves. Eventually we then put together the two solvers for a fluid-structure interaction simulation and a wave propagation test is carried out across the interface to determine whether the transmission of pressure wave across the interface follows the analytical solution. Once the wave propagation is validated against analytical results a single bubble collapse simulation was carried out. Figure 7 demonstrates a single bubble collapse simulation carried out by the SPH FSI cavitation solver. Figure 7 (a) shows the domain of the simulation where a bubble of radius 0.15 mm with its center placed at a distance of 0.2 mm from the interface is collapsed using a pressure wave of 50 MPa. Plastic strain developed in the material is shown in figure 7(c), the magnitude of plastic strain is however low (0.0012) and couldn't result in damage. So to produce enough plasticity to cause damage, multiple bubble collapse at the same point on the material is required, a single bubble collapse in the present case was not enough to cause damage.

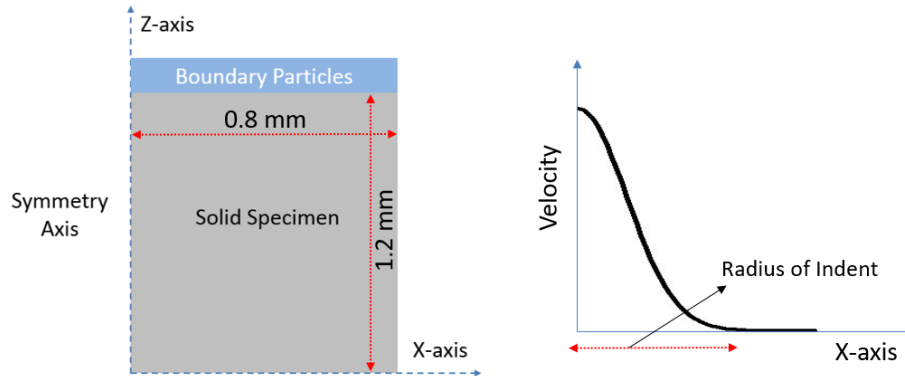


Figure 3. The figure on the left show the computational domain for solid simulation, the boundary particles marked in blue are given a downward velocity plotted on the right. (a Gaussian distribution is provided as the indent velocity as shown on the right, the radius of indent is defined as the distance from the center where the velocity is 1% of the peak value, a constant velocity is given to the indenter wrt time)

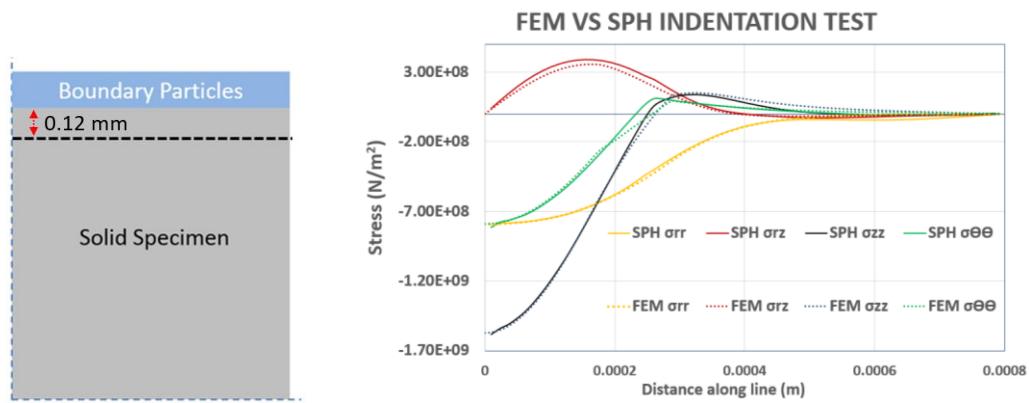


Figure 4. FEM results are compared against SPH for indentation of 6 microns in depth and 0.4 mm in radius for a stainless steel A-2205 specimen, the plots on right are plotted on the horizontal black dotted line (0.12 mm below the top surface) shown on the domain on the left.

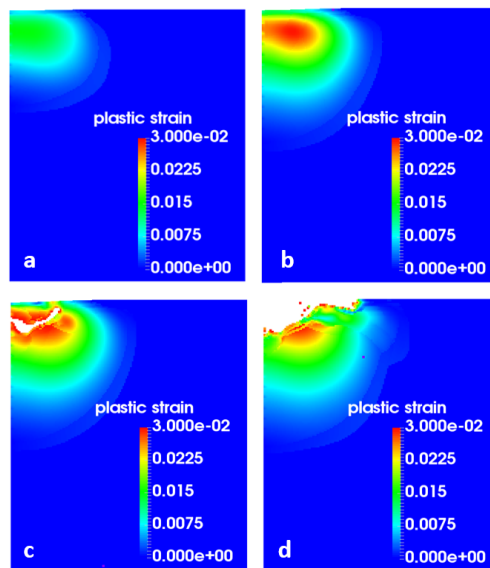


Figure 5. Sequence of images from damage simulation of a stainless steel A-2205 specimen, (a) Shows the plastic strain accumulation in material without damage, (b) high plastic strain zone just beneath the top surface, (c) damage initiation from the point of highest plastic strain, (d) material loss due to a single indent (domain size shown in the figure is same as in figure 3)

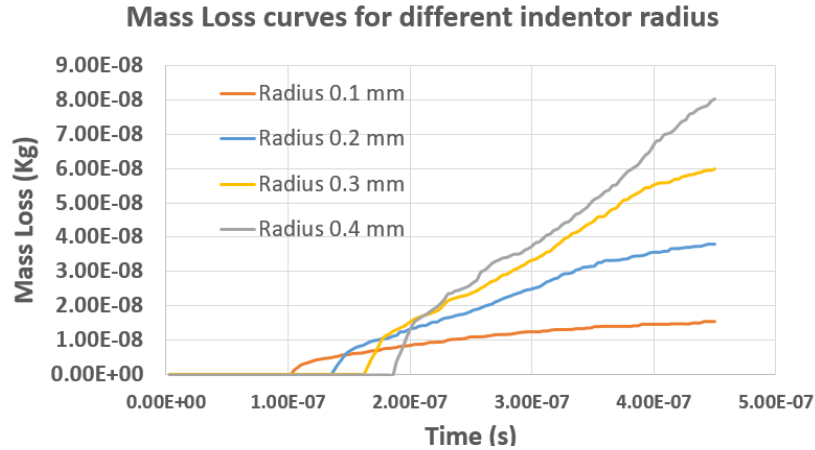


Figure 6. Mass loss curves for different indenter radius on a stainless steel A-2205 specimen obtained from SPH simulation, indentation depth is kept constant at 6 microns for all cases while the indenter radius is varied from 0.1 mm to 0.4 mm.

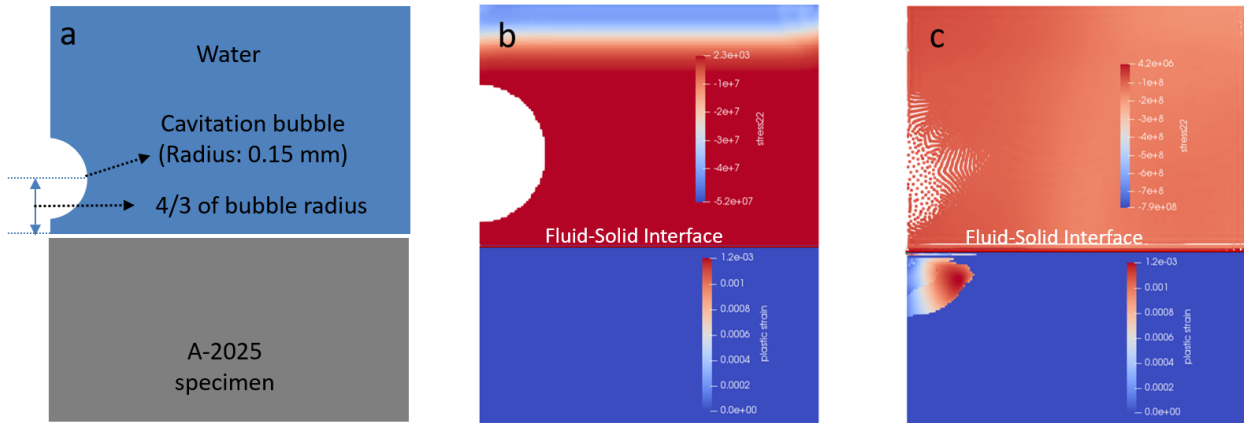


Figure 7. Fluid-structure interaction simulation of a bubble collapsing over a solid specimen: (a) Shows the computational domain for the simulation of a bubble of radius 0.15 mm with the center of the bubble at a distance of  $4/3$  times the radius from the interface, (b) SPH simulation where a pressure wave is generated from the top of the domain using repulsive particles producing a 50 MPa pressure wave approaching the bubble, (c) plastic strain developed in the material after the bubble collapse (contours in figure 7 (b) & (c) are for pressure in the fluid and plastic strain in the solid)

## Conclusion

A 2D axisymmetric fluid-structure interaction cavitation solver is developed. The fluid solver is used to simulate bubble collapse and a solid axisymmetric solver is used for solving elastic-plastic damage and material loss. The two solvers were put together to produce a fluid-structure interaction solver capable of solving a single bubble collapse near a solid surface.

Damage simulations were carried out to demonstrate the capability of the solver to solve for material damage. However, the damage criterion based on only plastic strain is simplistic. In reality the damage parameter should depend on three aspects [10]: Plastic strain, Triaxiality (the ratio of mean stress to von Mises stress which represents the pressure state of the material i.e. tension or compression) and deviatoric stress. Various predictive models have been proposed to determine fracture strains considering all the above parameters. However, using the above criteria leads to no damage in a single bubble collapse as shown in figure 7 since plastic strain is relatively low. To produce high plastic strain and therefore create damage needs multiple bubble collapse. The solver is presently being modified to accommodate multiple bubble collapse cases.

## References

- [1] A. Philipp, W. Lauterborn, Cavitation erosion by single laser-produced bubbles, *J. Fluid Mech.* 361, 1998, pp 75–116. doi:10.1017/S0022112098008738.J.
- [2] A. Vogel, W. Lauterborn, R. Timm, Optical and acoustic investigations of the dynamics of laser-produced cavitation bubbles near a solid boundary, *J. Fluid Mech.* 206 (1989) 299–338..
- [3] S.M. Ahmed, K. Hokkirigawa, R. Oba, Fatigue failure of SUS 304 caused by vibratory cavitation erosion, *Wear.* 177 (1994) 129–137. doi:10.1016/0043-1648(94)90238-0..
- [4] I.R. Jones, D.H. Edwards, An experimental study of the forces generated by the collapse of transient cavities in water, *J. Fluid Mech.* 7 (1960) 596–690. doi:10.1017/S0022112060000311..
- [5] T. Momma, A. Lichtarowicz, A study of pressures and erosion produced by collapsing cavitation, *Wear.* 186-187 (1995) 425–436. doi:10.1016/0043-1648(95)07144-X..
- [6] Par Francois Axisa, Jose Antunes, “Modelling of Mechanical Systems: Fluid-Structure Interaction,” 2007, Elsevier, ISBN 10: 0-7506-6847-4.
- [7] Gómez-Gesteira, M., Rogers, B.D., Dalrymple, R.A., Crespo, A.J.C. and Narayanaswamy, M., 2010, User Guide for the SPPhysics Code v2.0. <http://wiki.manchester.ac.uk/sphysics>
- [8] D. García-Senz, A. Relaño, R. M. Cabezón, E. Bravo, Axisymmetric smoothed particle hydrodynamics with self-gravity, *Monthly Notices of the Royal Astronomical Society*, Volume 392, Issue 1, 1 January 2009, Pages 346–360, 2008, <https://doi.org/10.1111/j.1365-2966.2008.14058.x>
- [9] G.R. Johnson, W.H. Cook, Fracture characteristics of three metals subjected to various strains, strain rates, temperature and pressure, *Engineering Fracture Mechanics*, Vol. 21, No. 1, pp. 31-48, 1985.
- [10] André Pineau, Amine A Benzerga, T Pardoen, Failure of metals I: Brittle and ductile fracture, *Acta Materialia*, Vol. 107, pp. 424-483, 2016.
- [11] <http://www-cast3m.cea.fr>